Proceedings World Geothermal Congress 2020+1
Reykjavik, Iceland, April - October 2021

Gravity, Transient Electro-Magnetic and Noise Seismic Exploration in the Puyuhuapi Geothermal Area, Southern Patagonia, Chile

Diego Aravena, Nicolás Pérez, Mauricio Muñoz, Karin García, Pablo Valdenegro, Bárbara Blanco, Diego Morata

Andean Geothermal Centre of Excellence, Universidad de Chile. Plaza Ercilla 803, Santiago, Chile.

daravena@ing.uchile.cl

Keywords: Gravity, Transient Electro-Magnetic, Seismic Noise, Nakamura, Puyuhuapi, Southern-Chile, Aysén region.

ABSTRACT

The Aysén region is located in Southern Patagonia, Chile (43°38′S to 49°16′S). It has optimum conditions for the formation of geothermal systems: magmatic processes, abundant rainfall and active faults systems (Negri et al., 2017 and references therein). The main structural feature in this region is the Liquiñe Ofqui Fault System (LOFS; Hervé 1976), composed of several NS to NNE major intra-arc dextral faults and many NE normal-dextral faults located in accommodation zones or faults-splay (Cembrano y Lara 2009). The LOFS is present between 39°S and 46°S latitude with several geothermal springs located along its borders.

A good prospect for high-enthalpy production is the Puyuhuapi Village. It is located in an N-S elongated basin, close to six hot-springs, nine minor eruptive centres and one of the major faults of the LOFS. Before a high-resolution geothermal prospection, it is necessary to precise some geological units to define geothermal targets.

We took 81 gravity measurement and 13 horizontal/vertical ratios of seismic noise (Nakamura, 1989) to understand the basin depth, density and impedance anomaly. Also, we measured seven Transient Electro-Magnetic (TEM) to constrain geological units and possible conductive bodies.

We modelled the gravity anomaly and observed an asymmetric-basin with a depocenter in the western part. Nakamura methodology also indicates the same asymmetric-shape with some variations. Uncoupling of the results inferred from the Nakamura and gravimetric methods varies from 30 to 50 m for most data. The uncoupling could be related to i) density contrast inside the basin, ii) S wave velocity variability within the basin and iii) an overestimation of the density contrast between the basins fill and basement (due to a fault damage zone).

TEM results do not show major conductive bodies inside the soil-basin, at least in the first 100 m depth. The results of all the geophysical methods suggest that hot spring manifestations are punctual anomalies related to fault systems. We suggest that the Puyuhuapi basin is a transition zone between the major NNE trending faults. Thus, emplacement of the PVG and the occurrence of thermal springs may be related to normal NE faulting allowing fluids to ascend. The existence of a geothermal reservoir is yet to be demonstrated.

1. INTRODUCTION

The Aysén region (43°38′S to 49°16′S) is located in an active plate margin associated with N76°E-trending subduction of the Nazca plates under the South American continental plate. Late subduction is evident by a series of Quaternary stratovolcanoes and monogenetic cones located along with fractures related to the Liquiñe Ofqui Fault System (LOFS). A major intra-arc dextral strike-slip fault system which runs from 39°S to 46°S (Cembrano et al., 1996, 2002; Cembrano and Hervé, 1993; Cembrano and Lara, 2009; Niemeyer et al., 1984). The LOFS is composed of major NS to NNE-striking dextral or dextral-reverse faults; and secondary NE-striking dextral to normal-dextral faults (e.g. Pérez-Flores, 2016). NE-faults are located in accommodation zones spatially associated with horse-tail fault systems, dilatational jogs and others splay-fault geometries. Structures in the study area coincide with a widespread fjord network formed by narrow channels and several islands, which separate the mainland from the adjacent Pacific Ocean (Bertrand et al., 2012).

The geology along the LOFS is dominated by the North Patagonian Batholith (NPB), a plutonic rock belt of 1000 km long and 200 km wide, emplaced during discrete episodes of magmatism from Late Jurassic to Late Cenozoic times (Pankhurst et al., 1999; Suárez and De la Cruz, 2001) (Figure 1a). In the vicinity of Puyuhuapi, the NPB comprises the Puyuhuapi Tonalite (14.4+-0.6 Ma; Cembrano et al., 2002) and the Risopatron Diorite (20.2+-2 Ma; Cembrano et al., 2002). Two Palaeozoic metamorphic complexes crop out west and east of the NPB (Figure 1a). Late Eocene to early Miocene marine volcano-sedimentary rocks of the Triaguén Formation (Hervé et al., 1995) is close to the study area. Hervé et al. (1995) proposed that these were deposited in pull-apart or asymmetric extensional basins in a transtensional setting along with a precursor to the present Liquiñe-Ofqui fault during a period of extremely oblique subduction.

Many thermal springs and eruptive centres are located in fractures along the NPB, in particular, the Puyuhuapi fjord has six identified thermal springs distributed along 45 km; in both coastal and inland areas (Fig. 1a). The Puyuhuapi Volcanic Group is a set of 9 Minor Eruptive Centres (MEC) located near the Puyuhuapi Village (Figure 1b); 4 centres are aligned along the north-western edge of the fjord (western alignment), four are aligned between the village and the Risopatron Lake (eastern alignment). Lahsen et al., 1994 suggests that the eruptive activity that produced the eastern alignment was probably subaquatic (phreatomagmatic) and that this activity dammed the Puyuhuapi fjord, creating the Risopatron Lake. An isolated centre is located six km south of the village. The eastern and western alignments have an N35ºE-trending direction and are separated by a distance of 2 km. Fluvial, glacio-fluvial and

landslide deposits of Holocene-Pleistocene age are the most important hydrogeological units located next to the Puyuhuapi Village (Figure 1c). Quaternary landslide deposits can also be observed on both sides of the valley (Figure 1c).

The region has optimum conditions for the formation of geothermal systems: the existence of magmatic processes (D'Orazio et al., 2003; Gutiérrez et al., 2005; Herve et al., 1995; Lahsen et al., 1994), abundant rainfall (~1200 mm/year) and active fault systems (Arancibia et al., 1999; Cembrano et al., 2002) that allow for deep circulation and rising of fluids. The objective of this work is to study the Puyuhuapi basins depth, density and impedance anomaly; by using gravity measurements and horizontal/vertical ratios of seismic noise. Additionally, we aim to constrain geological units and possible conductive bodies by using the Transient Electro Magnetic method. The results will be analysed in the light of their implications for geothermal exploration in the Puyuhuapi fjord.

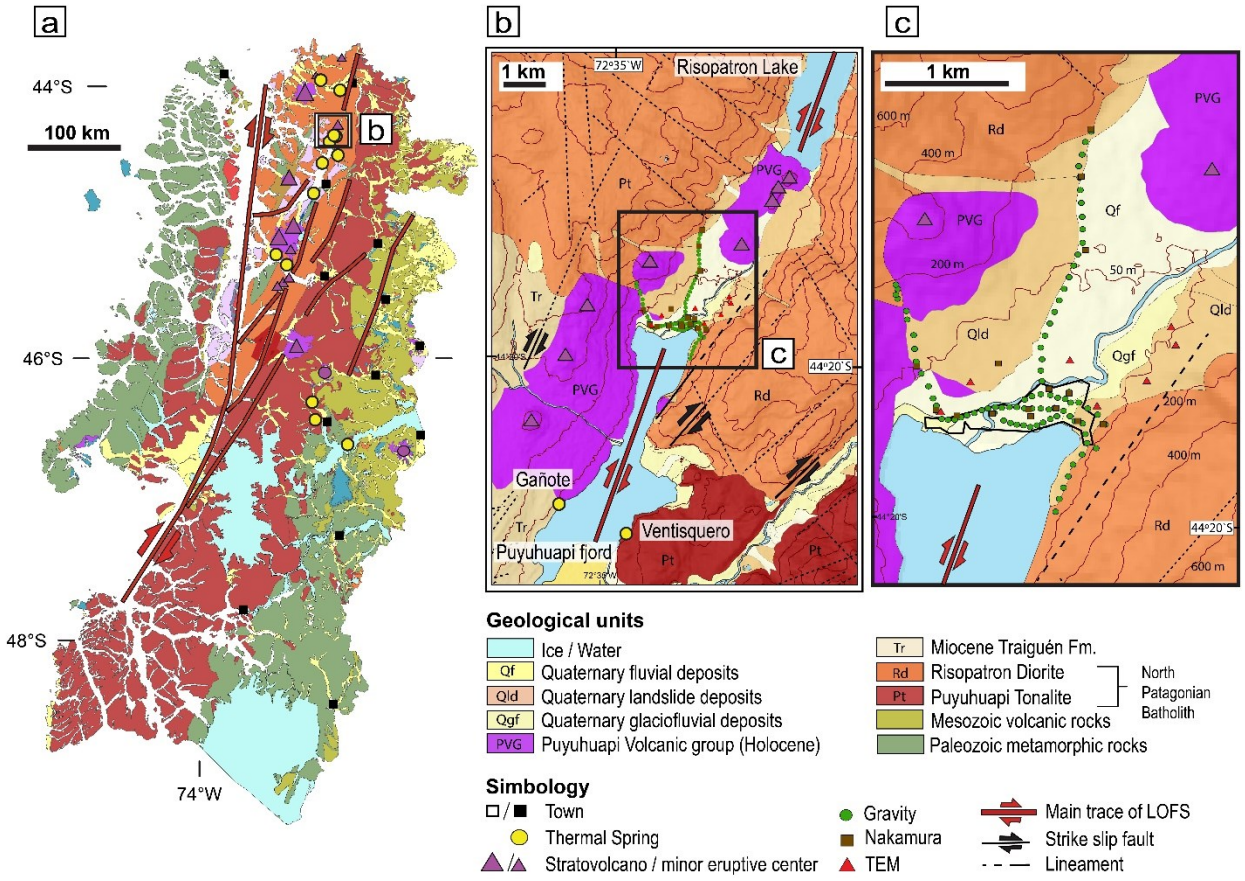

Figure 1: A) 1:500.000 Geological map of the Aysén region with the location of eruptive centres and thermal springs. (Niemeyer 1984; Lahsen et al., 1994; D'Orazio et al., 2003; Negri et al., 2017); B) 1:50.000 Geological map of the Puyuhuapi area (SERNAGEOMIN 2011); C) Close up to show geophysical data collected in this survey. Main structures modified from Lahsen et al. 1994; Arancibia et al., 1999; Cembrano et al., 1996 and SERNAGEOMIN 2011.

2. MATERIALS AND METHODS

2.1 Gravimetric survey

We took 81 gravity station widespread along with the Puyuhuapi town where roads were available, each one with a Gravity and DGPS measure. Specifically, one E-W profile was performed within the intrusive rock outcrops to understand the basin shape. Gravity measurement was carried out with the Scintrex CG-5 gravimeter. We took two time-window series of 60 seconds at each station and chose the data with less standard deviation. Only data with an error below 0.1 mGals were saved. To obtain accurate elevation, we use Trimble R4 DGPS, with a base station at the same town. Vertical position errors were always below 20 cm, mean vertical error is 4.3 cm with a standard deviation of 6.1 cm (0.012 ± 0.019 mGals error in free-air gravity correction). Absolute gravity was calculated eliminating the daily derive, and the Tidal correction. To obtain the basin anomaly, we subtract the Latitude, Free-Air, Bouguer and Terrain corrections. For more details of this methodology and data reduction, refer to Telford et al. (1990). A 1D inversion was programmed in MATLAB considering a Bouguer anomaly and using the density of intrusive rocks and lavas measured on the field.

2.2 Nakamura survey

We took 13 measurements of the horizontal/vertical spectral ratio of seismic noise around the Puyuhuapi Village, to define the sedimentary thickness, and compare the gravity modelling from another physical approach. This methodology was carried out with a three-component seismometer TROMINO, recording 30 minutes of ambient noise.

To estimate the sedimentary thickness, we use formula (1):

$$H = Vs/4f \quad (1)$$

Where "H" is the sedimentary thickness; "Vs" is the shear-wave velocity of the soil and "f" in the peak frequency of the H/V spectral curve. From the ambient noise record, we take a time-window of 30 seconds and calculate the H/V curve. Thus, for each Nakamura point, we obtain 60 H/V curve allowing to constrain "f" statistically. Shear wave velocity of the sedimentary basin was constrained from the literature as 270 m/s (Zaslavisky 2012; Gorstein & Ezersky, 2015). Further details regarding this methodology can be found in Nakamura (1989).

2.3 Transient Electro-Magnetic (TEM) Survey

TEM stations were deployed around the Puyuhuapi town, where the unurbanised field was available. Stations are composed of two cable-loops to induce a magnetic field in the ground (Transmission loop "Tx") and measure the electrical response of the site (Receiver loop "Rx"). Transmission loops are square of 40x40 meters or 100x100 meters, depends on the available site dimension. Receiver loops are square cables of 5x5m for the smaller Tx, and 10x10 for the bigger Tx. WalkTem ABEM equipment was used for data acquisition. In total, eight stations were carried out as it is observable in Figure 1c. To process the time-series obtained in the data acquisition, we use the Interpex, IX1Dv3 software, specifically to data processing and data modelling.

3. RESULTS

Figure 2a shows the residual gravity anomaly obtained in the study area. There seems to be a negative gravimetric anomaly in the middle of the basin that can be observed in the EW and the NS gravity transects. Lower residual anomalies observed in both transects suggest an N35°E elongated depocenter. Figure 3 and Figure 4 resume the main results obtained in this work with the three methods. The inferred basin thickness varies from 0 m depth on both extremes of the section, were gravity data was obtained directly on top of intrusive rock outcrops; up to 200 m depth in the middle part of the basin, below the western part of the town. Gravity data also suggest a slightly asymmetric shape of the basins central part, with its western and eastern sides dipping 48º and 58º respectively (section DE, **Error! Reference source not found.**) and its main axis oriented N30°E (yellow contours in Figure 3). The width of the basin reaches ~2.300 m when measured perpendicular to the main axis.

Depth of the basin as inferred from Nakamura measurements suggests a shallower basement in almost all points when compared with gravity results (except measurement N5) with the basin depth varying from 12 to 147 meters (Figure 4a). They also show different coherence when related to the gravity data; measurements N1, N2 and N5 have less than 30 m of displacement respect to the gravity inversion, measurements N6, N7 and N8 have 40 to 50 m of displacement. (Figure 4a) The datum N3 was measured in a permanent seismic station which has a longer measurement time and better resolution, allowing to identify two peaks in the H/V spectral curve at 4.46 Hz and ~7 Hz (Figure 2b).

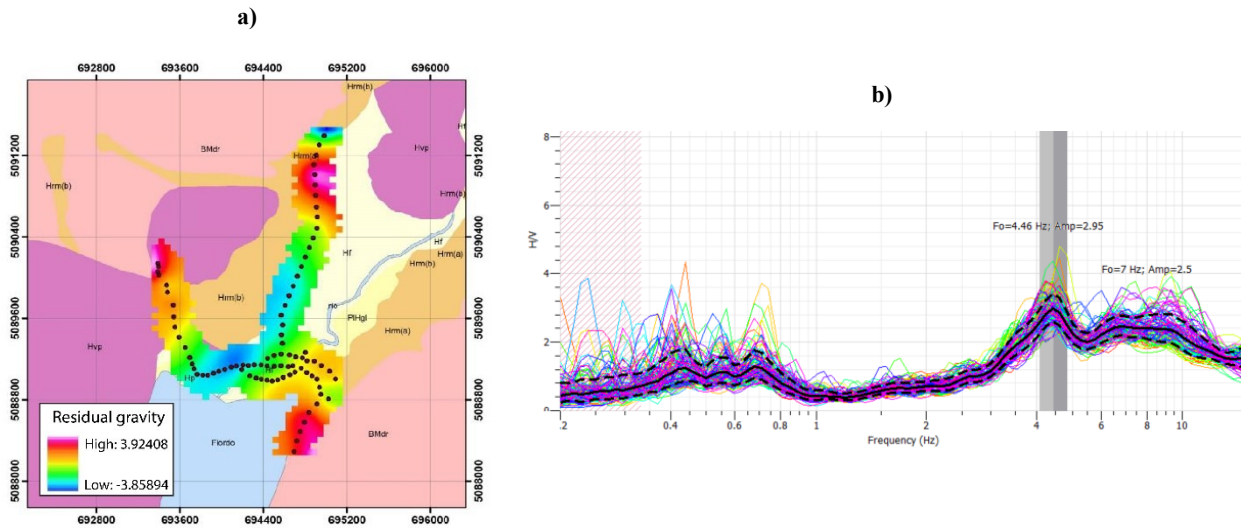

Figure 2: a) Residual gravity anomaly. b) Nakamura results as Frequency vs H/V spectral curve for the N3 seismic station. L=30 s; number of cycles=115. Two peaks can be differentiated at 4.46 Hz and 7 Hz, related to depths of 9 m and 89 m respectively.

The resistivity modelled from TEM data show three configurations (Figure 4a):

- TEMs 1 and 2 adjust to a 3-layer-model with a shallow, slightly resistive, upper layer (~30 Ωm, 6 m thick). Underneath this layer, there is a 71 m thick, highly resistive layer (~2000 Ωm). Below the resistive layer; TEM 1 shows a highly conductive layer (~2 Ωm, 7 m thick). This layer is not observed in TEM 2 was a 50 Ωm, 131 m thick layer, is obtained in the inversion process.

- TEM 5 is located near intrusive rock outcrops and shows a single layer with a thickness of 150 m and a resistivity of 331 Ωm.

- TEM 6 is located nearly 500 m north of the ABC section. Inversion of data shows a 23 Ωm, 49 m thick layer; underneath this layer, there is a 16 m thick conductive layer (2 Ωm), followed by a 25 Ωm layer with undetermined thickness.

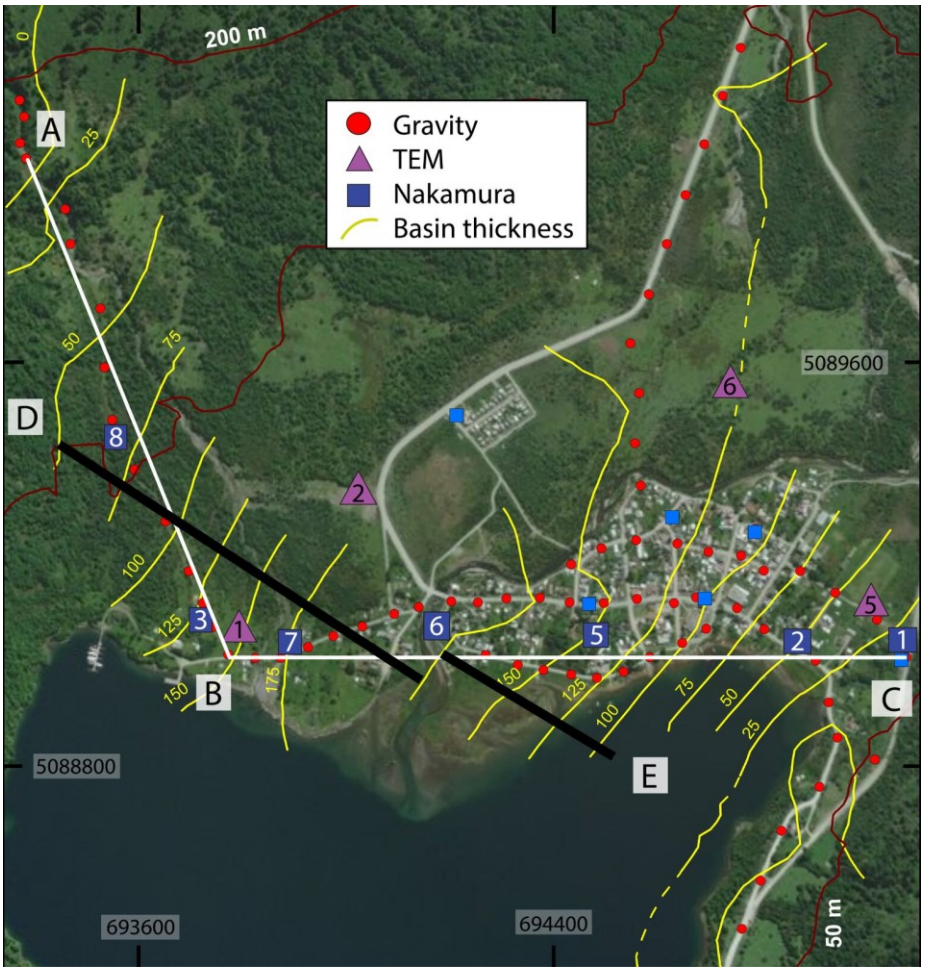

Figure 3: Satellite image of the Puyuhuapi town with identification and location of gravity, Nakamura and TEM measurements. Yellow curves indicate the inferred basin thickness if an intrusive basement is considered. Small blue squares area Nakamura data that is not included in this study yet.

4. DISCUSSION

Uncoupling of the results inferred from the Nakamura and gravimetric methods varies from 30 to 50 m for most data. The uncoupling could be related to i) density contrast inside the basin, ii) S wave velocity variability within the basin and iii) an overestimation of the density contrast between the basins fill and basement (due to a fault damage zone). Nevertheless, the N3 datum (Figure 2a), which has a longer measurement time and better resolution, allows the identification of two peaks in the H/V spectral curve at 4.46 Hz and 7 Hz. If a Vs of 270 m/s and 1800 m/s are assumed for the basin fill and basement respectively, then the two peaks observed in Figure 2b can be modelled as two levels of velocity contrast, located at 9 m and 89 m depth respectively (N3a and N3b respectively in Figure 4a). This estimation correlated well with the TEM's inversion (Figure 4a). The thickness inferred in N3a and N3b has a good correlation with a 60-70 m thick resistive body observed in TEM 1 and TEM 2 (section ABC, Figure 4). We suggest these observations can be explained by the presence of lavas beneath the western side of the basin; if such assertion is true, then the gravity basin depth of the basin would be underestimated due to a lower density of the lavas when compared with the intrusive basement measured in the field (2.39 g/cm^3 v/s 2.71 g/cm^3, respectively). The dashed black line in section ABC (Figure 4) shows the modelled depth of the basement if we use the density of lavas instead of intrusive rocks in the western side of the basin applying the Bouguer plate approximation. The difference may increase the modelled basin depth by a factor of two.

The TEM 1 shows a highly conductive body (2 Ωm) just underneath the interpreted lavas, we suggest this response to a saline intrusion of fjord water that could be intruding through the base of the lavas. Even though TEM 6 also shows a two Ωm conductive

body, it is located too far from the shore to be explained by a saline intrusion (~500 m). We suggest it could be explained by the presence of water-saturated clays of glacial origin.

The orientation of the basins main axe (N35°E) is compatible with previous structural analyses that describe NE dextral normal faults, and NS to NNE dextral reverse faults in the Puyuhuapi area (Lahsen et al., 1994; Arancibia et al., 1999). The asymmetric shape of the basins central part, with its western and eastern sides dipping 48º and 58º respectively (section DE, **Error! Reference source not found.**), suggests a structural control. According to with the paleo-stress inversion obtained from faults striae, the stress distribution of the area has an N52°E/6°E shortening direction (Lavenu & Cembrano 1999), with a transpressional tectonic environment (e.g. Lavenu & Cembrano 1999; Cembrano et al. 2002). In this tectonic context, it is expected that major NNE faults behave as dextral to reverse-dextral faults, and NE-trending faults behaves as dextral to normal-dextral faults (e.g. Rosenau 2006, Perez-Flores 2016). Since the gravity anomaly suggest that the Puyuhuapi basin depocenter has an N35°E orientation, we infer a tectonic control by dextral to normal-dextral faults. This trending direction is also observable in the lineaments formed by minor eruptive centres (N35°E), as well as fractures controlling some lava flows of the PVG (N40°E; Lahsen et al. 1994). Two thermal springs are located on the southern edge of the PVG, Gañote and Ventisquero (Figure 1b), whose estimated reservoir temperature by silica geothermometry range from 142 to158 ºC at depth (Negri et al., 2017), evidencing a close relationship between structural, hydrothermal and magmatic activity.

North and south of the village, geomorphological lineaments and exhumed fault planes indicate the occurrence of ~N10°E trending faults with a separation of ~500-1000 meters in an E-W direction. We suggest that the Puyuhuapi basin is a transition zone between the major NNE trending faults. Thus, emplacement of the PVG and the occurrence of thermal springs may be related to normal NE faulting allowing fluids ascension.

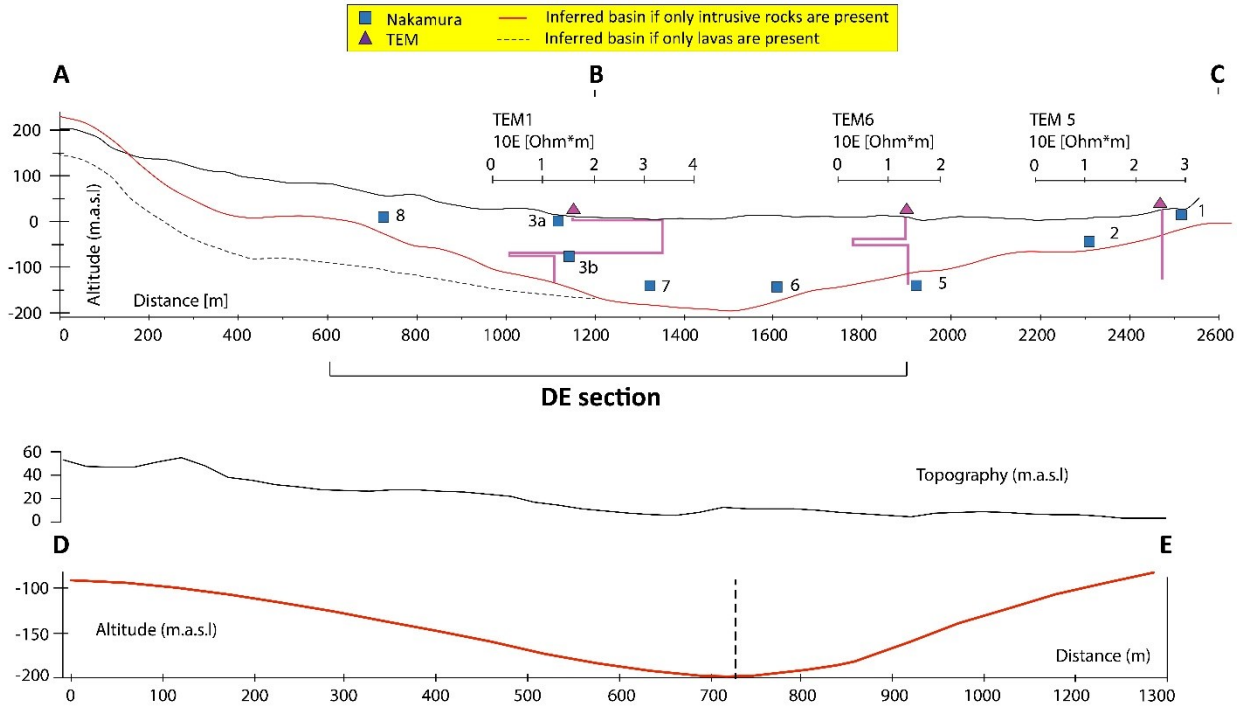

Figure 4: ABC and DE cross sections depicting the main results obtained in this work. Location of sections can be seen in Figure 3. Thick purple lines beneath the TEMs indicate the modelled resistivity.

5. CONCLUSIONS

The TEM results infer the presence and thickness of a lava flow on the western side of the basin. They also show two strong conductive bodies: one located close to the shore, interpreted as a saline intrusion; and a second conductive body located inland and interpreted as a small lens of water-saturated clay.

We modelled the gravity anomaly and inferred a slightly asymmetric basin with an N35ºE trending depocenter that reaches 200m of thickness. The observed geometry suggests a structural control of the shape of the basins. Nakamura methodology also suggests the same asymmetric-shape, but the interpreted depth of the basin is 30m to 50m shallower when compared to gravity. The difference between both anomalies can be related with i) density contrast inside the basin, ii) S wave velocity variability within the basin and iii) an overestimation of the density contrast between the basins fill and basement (due to a fault damage zone).

We suggest that the Puyuhuapi basin is a transition zone between the major NNE trending faults. Thus, emplacement of the PVG and the occurrence of thermal springs may be related to normal NE faulting allowing fluids ascension. The existence of a geothermal reservoir is yet to be demonstrated.

REFERENCES

Arancibia, G., Cembrano, J., & Lavenu, A. (1999). Transpresión dextral y partición de la deformación en la Zona de Falla Liquiñe-Ofqui, Aisén, Chile (44-45ºS). Revista geológica de Chile, 26(1), 03-22.

Bertrand, S., Hughen, K.A., Sepulveda, J., Pantoja, S., 2012. Geochemistry of surface sediments from the fjords of Northern Chilean Patagonia (44−47°S): spatial variability and implications for paleoclimate reconstructions. Geochim. Cosmochim. Acta 76, 125–146.

Cembrano, José, and Francisco Herve. "The Liquine Ofqui Fault Zone: A major Cenozoic strike slip duplex in the southern Andes." (1993): 175-178.

Cembrano, José, Francisco Hervé, and Alain Lavenu. 1996. “The Liquiñe Ofqui Fault Zone: A Long-Lived Intra-Arc Fault System in Southern Chile.” Tectonophysics 259 (1). Elsevier: 55–66.

Cembrano, José, Alain Lavenu, Peter Reynolds, Gloria Arancibia, Gloria López, and Alejandro Sanhueza. "Late Cenozoic transpressional ductile deformation north of the Nazca–South America–Antarctica triple junction." Tectonophysics 354, no. 3-4 (2002): 289-314.

Cembrano, J., Lara, L., 2009. The link between volcanism and tectonics in the southern volcanic zone of the Chilean Andes: a review. Tectonophysics 471, 96–113.

D'Orazio, Massimo, Fabrizio Innocenti, P. Manetti, Marco Tamponi, S. Tonarini, Oscar González-Ferrán, A. Lahsen, and R. Omarini. "The Quaternary calc-alkaline volcanism of the Patagonian Andes close to the Chile triple junction: geochemistry and petrogenesis of volcanic rocks from the Cay and Maca volcanoes (∼ 45 S, Chile)." Journal of South American Earth Sciences 16, no. 4 (2003): 219-242.

Fang, Z., Boucot, A., Covacevich, V., Herve, F., 1998. Discovery of late Triassic fossils in the Chonos metamorphic complex, southern Chile. Rev. Geol. Chile 25, 165–173.

Gorstein, M., & Ezersky, M. 2015. Combination of HVSR and MASW Methods to Obtain Shear Wave Velocity Model of Subsurface in Israel. International Journal of Geohazards and Environment, 20–41. https://doi.org/10.15273/ijge.2015.01.004

Gutiérrez, F., Gioncada, A., Ferran, O. G., Lahsen, A., & Mazzuoli, R. (2005). The Hudson Volcano and surrounding monogenetic centres (Chilean Patagonia): an example of volcanism associated with ridge–trench collision environment. Journal of Volcanology and Geothermal Research, 145(3-4), 207-233.

Hervé, M. 1976. “Estudio Geológico de La Falla Liquiñe-Reloncaví En El área de Liquiñe; Antecedentes de Un Movimiento Transcurrente (Provincia de Valdivia).” In Congreso Geológico Chileno. Vol. 1.

Hervé, F., Godoy, E., Garrido, I., Hormazábal, L., Brook, M., Pankhurst, R.J., Vogel, S., 1988. Geocronologia y condiciones de metamorfismo del complejo de subduccion del archipielago de los Chonos. Congreso Geológico Chileno 5.

Herve, F., Pankhurst, R.J., Drake, R., Beck, M.E., 1995. Pillow metabasalts in a mid-Tertiary extensional basin adjacent to the Liquiñe-Ofqui fault zone: the Isla Magdalena area, Aysen, Chile. J. S. Am. Earth Sci. 8, 33–46.

Herve, F., Fanning, C.M., 2001. Late Triassic detrital zircons in meta-turbidites of the Chonos Metamorphic Complex, southern Chile. Rev. Geol. Chile 28, 91–104.

Lahsen, A., López Escobar, L., Vergara, M., 1994. The Puyuhuapi volcanic group, Southern Andes (44°20′S): geological and geochemical antecedents. In: 7 Congreso Geológico Chileno. 11. Chile, Concepción, pp. 1076–1079.

Nakamura, Y. (1989). A method for dynamic characteristics estimation of subsurface using microtremor on the ground surface. Railway Technical Research Institute, Quarterly Reports, 30(1).

Negri, A., Daniele, L., Aravena, D., Munoz, M., Delgado, A., & Morata, D. (2018). Decoding fjord water contribution and geochemical processes in the Aysen thermal springs (Southern Patagonia, Chile). Journal of Geochemical Exploration, 185, 1-13

Niemeyer, H., Skarmeta, J., Fuenzalida, R., Espinosa, W., 1984. Hojas Península de Taitao y Puerto Aisén. Región de Aisén del General Carlos Ibañez del Campo. Escala 1:500.000. In: Servicio Nacional de Geología y Minería.

Pankhurst, R.J., Weaver, S.D., Hervé, F., Larrondo, P., 1999. Mesozoic-Cenozoic evolution of the North Patagonian batholith in Aysen, southern Chile. J. Geol. Soc. Lond. 156, 673–694.

SERNAGEOMIN. 2003. “Mapa Geológico de Chile: Versión Digital.” Mapa Geológico de Chile: Versión Digital. Santiago: Servicio Nacional de Geología y Minería.

SERNAGEOMIN, 2011. Investigación Geológica Minera Ambiental en Aysen.

Suárez, M., De la Cruz, R., 2001. Jurassic to Miocene K-Ar dates from eastern central Patagonian Cordillera plutons, Chile (45°−48°S). Geol. Mag. 138, 53–66.

Telford, W. M., Geldart, L. P., and Sheriff, R. E. (1990) Applied Geophysics, Cambridge University Press, UK, 1–770.

Zaslavsky, Y., Shapira, A., Gorstein, M., Perelman, N., Ataev, G., & Aksinenko, T. 2012. Questioning the applicability of soil amplification factors as defined by NEHRP (USA) in the Israel building standards. Natural Science, *04*. https://doi.org/10.4236/ns.2012.428083